Electronic Supplementary Material (ESI) for Polymer Chemistry.
This journal is © The Royal Society of Chemistry 2018

Electronic supplementary information

A 1,2,3-triazolyl based conjugated microporous polymer for sensitive detection of *p*-nitroaniline and Au nanoparticles immobilization

Feng Wei,‡ Xinyi Cai,‡ Junqi Nie*, Feiyi Wang, Cuifen Lu, Guichun Yang, Zuxing Chen, Chao Ma and Yuexing Zhang*

Hubei Collaborative Innovation Center for Advanced Organochemical Materials & Ministry-of-Education Key Laboratory for the Synthesis and Application of Organic Functional Molecules, Hubei University, Wuhan 430062, China

E-mail: jqnie@hubu.edu.cn, zhangyuexing@sdu.edu.cn

1. Experimental Section

Synthesis of 1,3,5-tris(1-(3,5-di(thiophen-2-yl)phenyl)-1H-1,2,3-triazol-4-yl)benzene (TPTB)

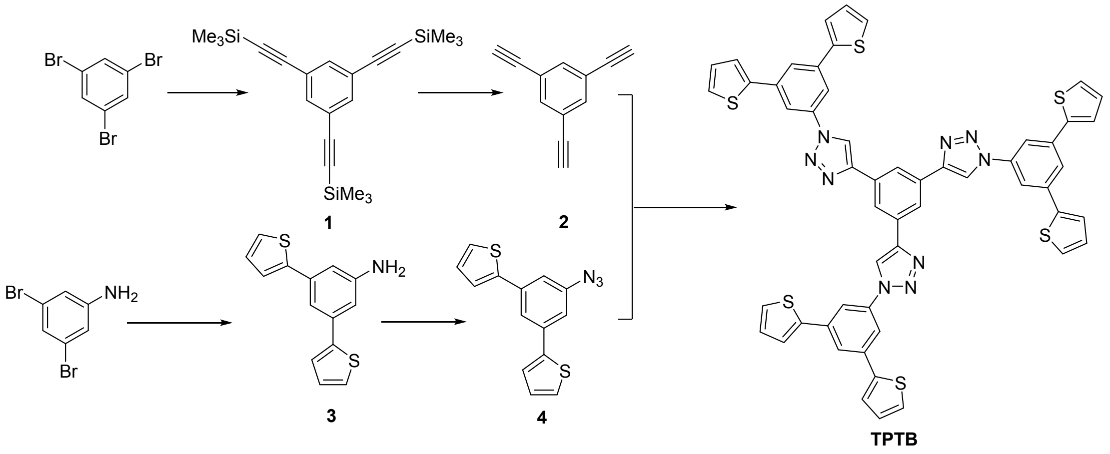

a. Synthesis of 2

The product was synthesized by the previous procedure [S1]. 1,3,5-Tribromobenzene (0.5 g, 1.6 mmol), tetrakis(triphenylphosphine) palladium (0.184 g, 0.16 mmol) and CuI (0.025 g, 0.13 mmol) were dissolved in dry triethylamine (4 mL) and toluene (4 mL) and then (trimethylsilyl)acetylene (0.89 mL, 6.3 mmol) was added. The mixture was stirred under a nitrogen atmosphere at 90 °C overnight. After cooling to room temperature, the reaction mixture was filtered and the filtrate was concentrated under reduced pressure to give crude **1**. Then **1** was suspended in tetrahydrofuran (5 mL) and methanol (5 mL), and a aqueous KOH solution (1 M, 5 mL) was added dropwise. The mixture was stirred at room temperature for 1 hour and extracted with dichloromethane (15 mL × 3). The combined organic extracts were washed with H_2O and dried over anhydrous $MgSO_4$. The volatiles were removed under vacuum to give crude product, which was purified by column chromatography on silica gel (petroleum ether) to obtain **2** as light a yellow powder. Yield: 0.21 g (88%). ^{1}H NMR (600 MHz, $CDCl_3$) δ 7.57 (s, 3H), 3.11 (s, 3H).

b. Synthesis of 3

A mixture of 3,5-Dibromonitrobenzene (1.433 g, 5.71 mmol), 2-tributylstannylthiophene (4.54 mL, 14.28 mmol) and tetrakis(triphenylphosphine) palladium (0.66 g, 0.57 mmol) in 25 mL anhydrous toluene was heated at 110 °C for 24 h under nitrogen atmosphere. After cooling to room temperature, the mixture was added water (25 mL) and the aqueous layer was extracted with dichloromethane (50 mL × 3). The combined organic layers were dried over anhydrous $MgSO_4$. The volatiles were removed under vacuum to give crude product, which was purified by column chromatography on silica gel (petroleum ether/dichloromethane = 5/1) to obtain **3** as a white solid. Yield: 1.19 g (81%). ^{1}H NMR (600 MHz, $CDCl_3$) δ 3.80 (s, 2H), 6.86 (d, *J* = 6.0 Hz, 2H), 7.09 (dd, *J* = 5.4 Hz, 2H), 7.29 (dd, *J* = 4.2 Hz, 3H), 7.33 (dd, *J* = 5.4 Hz, 2H); ^{13}C NMR (150 MHz, $CDCl_3$) δ 147.21, 144.21, 135.99, 127.92, 124.86, 123.38, 114.56, 111.88. MALDI-TOF (m/z): calcd for $C_{14}H_{12}NS_2$ 258.0406 $[M + H]^+$, found 258.0403.

c. Synthesis of 4

In a round-bottom flask equipped with a magnetic stirring bar, **3** (2.574 g, 10 mmol) was dissolved in HCl (6N, 10 mL) in an ice bath. Then 25 mL of aqueous solution of sodium nitrite (1.035 g, 15 mmol) was added dropwise. The reaction mixture was stirred for 0.5 h and 50 mL of aqueous solution of sodium azide (2.6 g, 40 mmol) was added dropwise. After addition, the mixture was allowed to stir for another 24 hours at room temperature. Then the mixture was extracted with ethyl acetate and the combined organic extracts were washed with H_2O and dried over anhydrous $MgSO_4$. The volatiles were removed under vacuum to give crude product, which was purified by column chromatography on silica gel (petroleum ether) to obtain **4** as a yellow solid. Yield: 2.58 g (91%). ^{1}H NMR (600 MHz, $CDCl_3$) δ 7.60 (t, *J* = 1.8 Hz, 1H), 7.38 (dd, *J* = 3.6 Hz, 2H), 7.34 (dd, *J* = 5.4 Hz, 2H), 7.16 (d, *J* = 1.8 Hz, 2H), 7.11 (q, *J* = 3.6 Hz, 2H); ^{13}C NMR (150 MHz, $CDCl_3$) δ 142.82, 141.24, 136.65, 128.18, 124.17, 120.27, 115.27. MALDI-TOF (m/z): calcd for $C_{14}H_{10}N_3S_2$ 284.0311 $[M + H]^+$, found 284.0307.

d. Synthesis of TPTB

2 (0.204 g, 1mmol), **4** (1.383 g, 4.88 mmol), $CuSO_4 \cdot 5H_2O$ (0.105 g, 0.42 mmol) and sodium ascorbate (0.083 g, 0.42 mmol) in dry DMF (60 mL) was stirred under a nitrogen atmosphere at 100 °C for 36 h. After cooling to room temperature, 100 mL of methyl tert-butyl ether was added to the reaction mixture. The resulting precipitate was filtered and subsequently washed with water, ethanol, and dichloromethane to remove any unreacted monomers or residues. The solid was dried in vacuo at 60 °C for 12 h to give the product as a light yellow powder. Yield: 1.12 g (82%). ^{1}H NMR (600 MHz, DMSO-d_6) δ 9.76 (s, 3H), 8.65 (s, 3H), 8.25 (s, 6H), 8.02 (s, 3H), 7.86 (s, 6H), 7.72 (s, 6H), 7.27 (s, 6H); ^{13}C NMR (150 MHz, $CDCl_3$) δ 147.47, 142.02, 138.56, 136.95, 132.36, 129.03, 127.42, 126.06, 122.84, 120.97, 116.33. MALDI-TOF (m/z): calcd for $C_{54}H_{33}N_9S_6Na$ 1022.1075 $[M + Na]^+$, found 1022.1072.

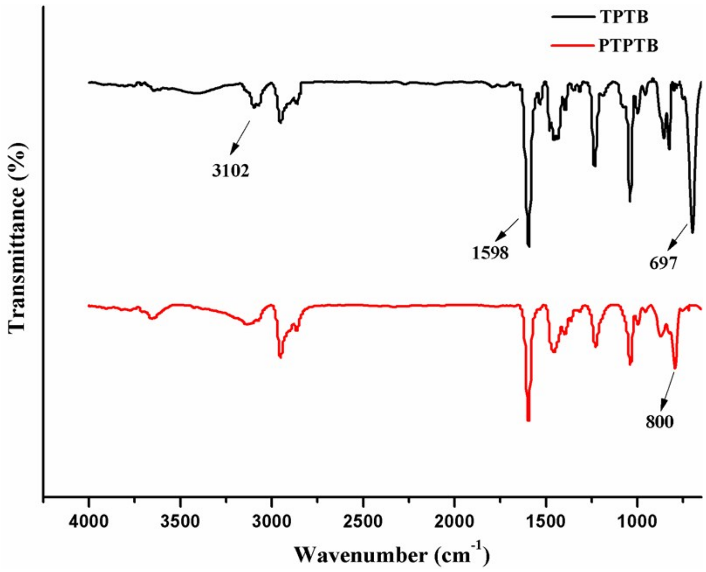

Figure S1 FT-IR spectra of TPTB and PTPTB.

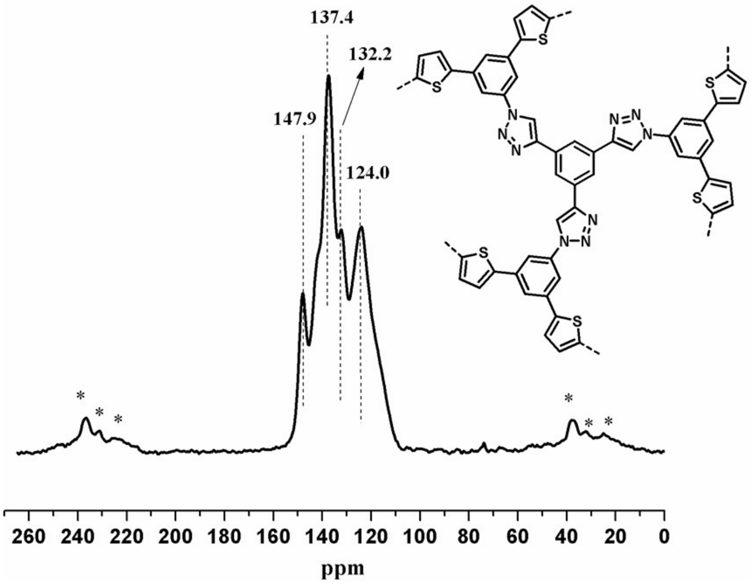

Figure S2 Solid-state ^{13}C NMR spectra for PTPTB. Asterisk denotes spinning sidebands.

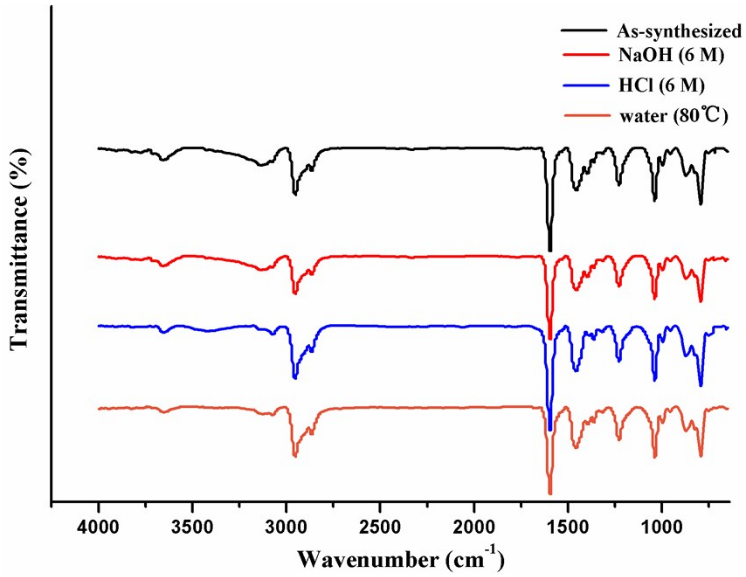

Figure S3 FT-IR spectra of PTPTB samples upon treatment in different solvents.

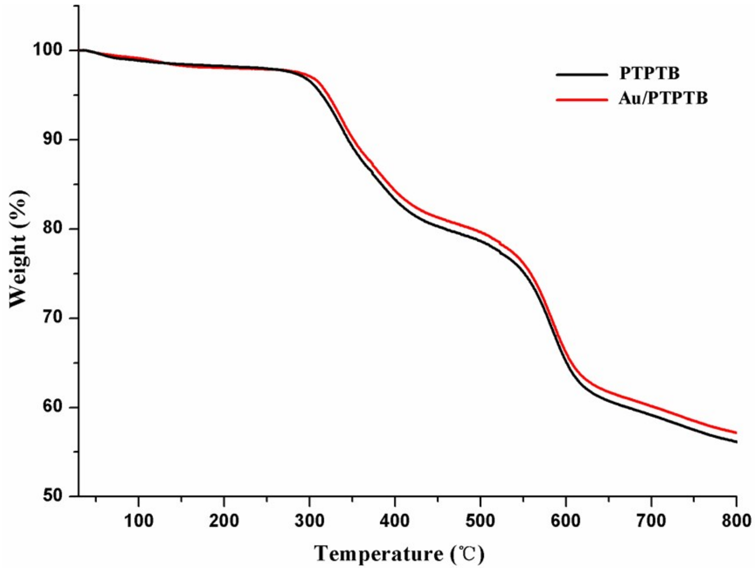

Figure S4 TGA curves of PTPTB and Au/PTPTB.

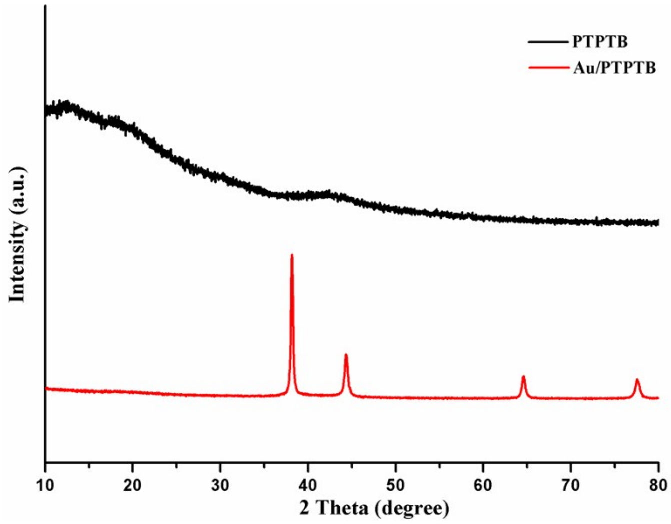

Figure S5 PXRD patterns of PTPTB and Au/PTPTB.

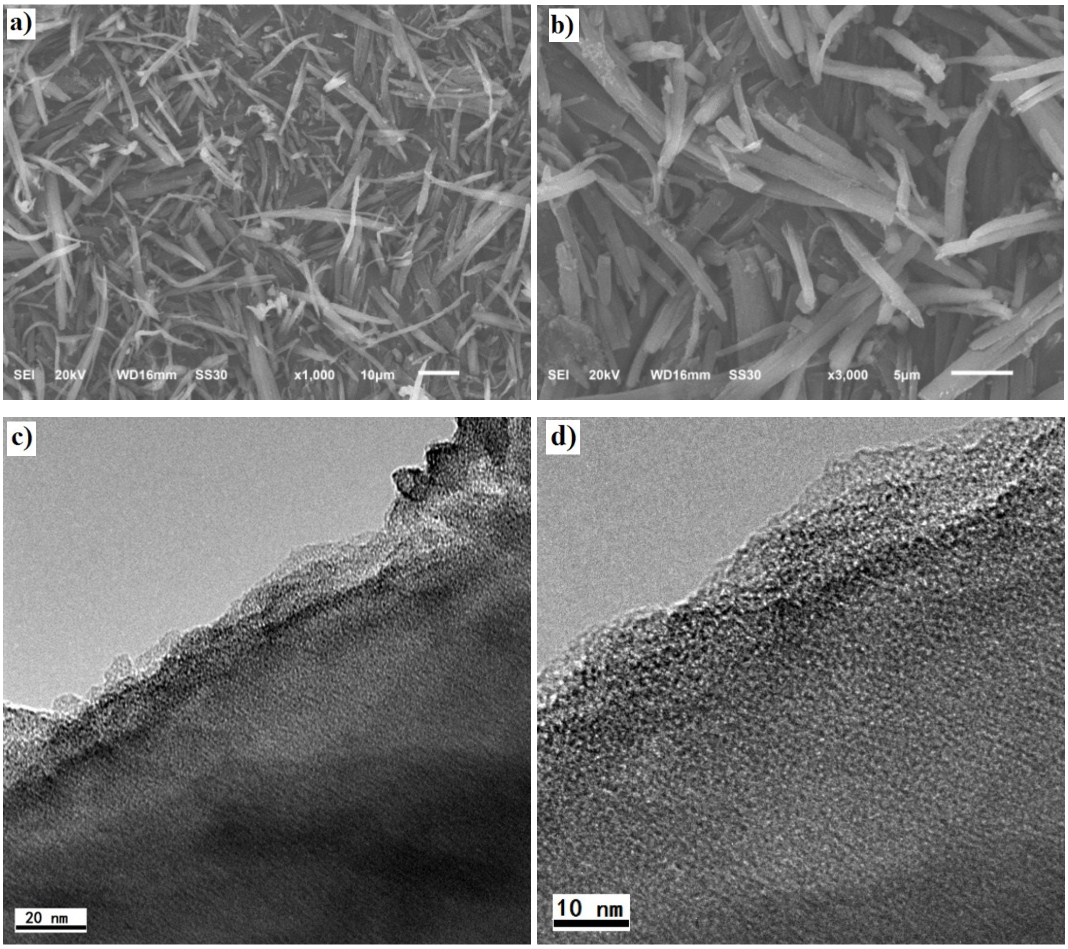

Figure S6 SEM (a, b) and TEM (c, d) images of PTPTB.

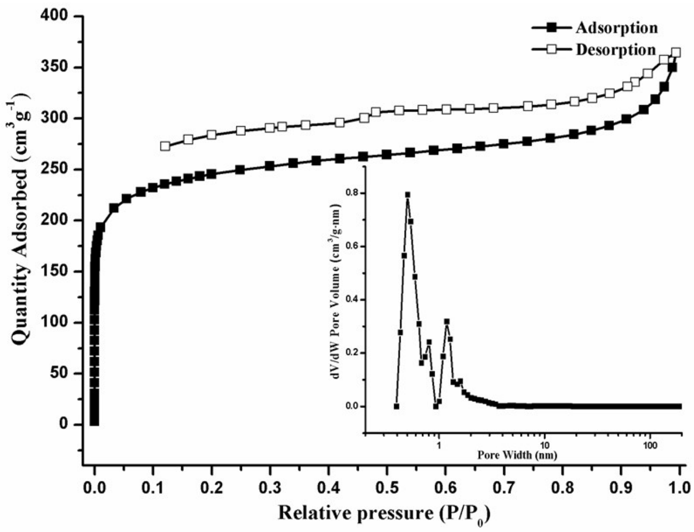

Figure S7 Nitrogen sorption isotherms of PTPTB. Inset: pore-size distribution profile calculated by using the DFT method.

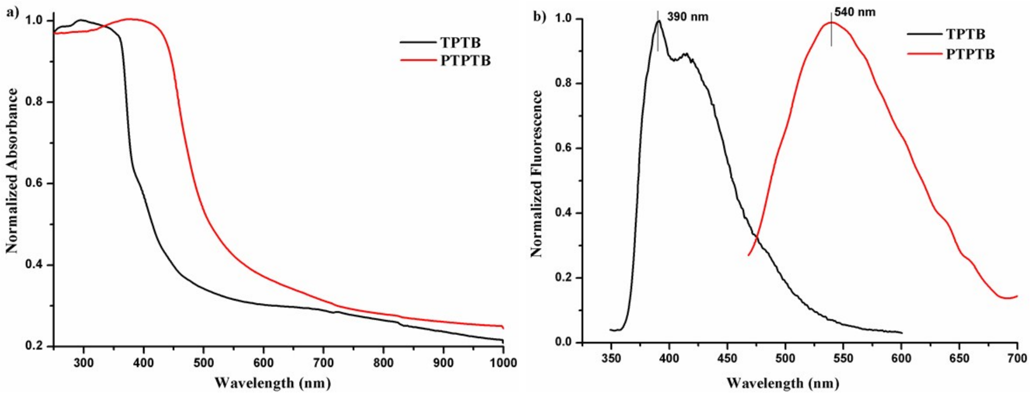

Figure S8 (a) Diffuse reflectance UV-Vis spectra of TPTB and PTPTB. (b) Fluorescence spectra of TPTB and PTPTB.

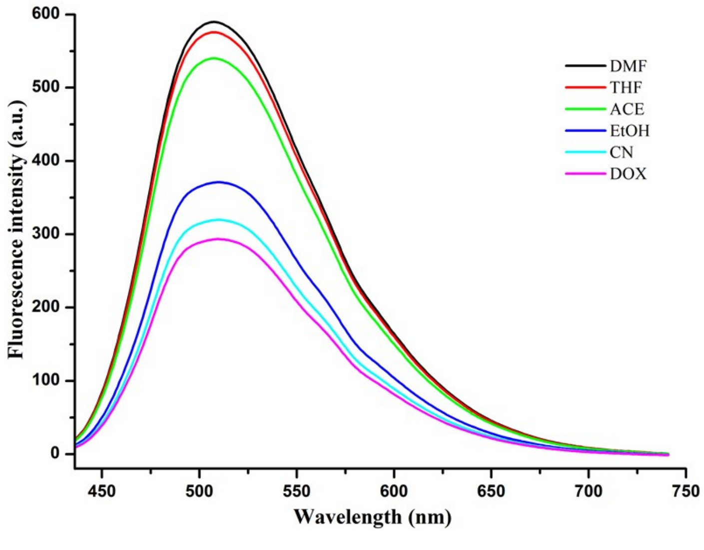

Figure S9 Emission spectra of PTPTB dispersed in different solvent (λ_{ex} = 417 nm).

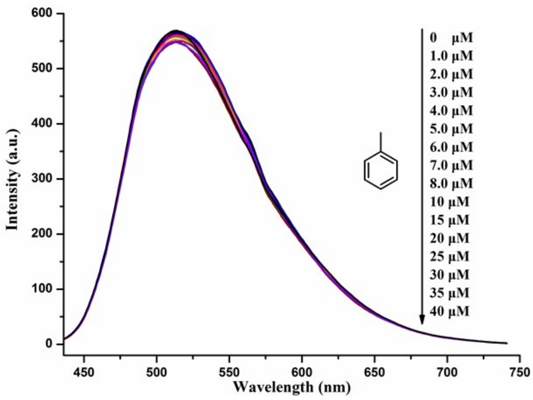
Intensity (a.u.)
Wavelength (nm)
0
100
200
300
400
500
600
450
500
550
600
650
700
750
0 μM
1.0 μM
2.0 μM
3.0 μM
4.0 μM
5.0 μM
6.0 μM
7.0 μM
8.0 μM
10 μM
15 μM
20 μM
25 μM
30 μM
35 μM
40 μM

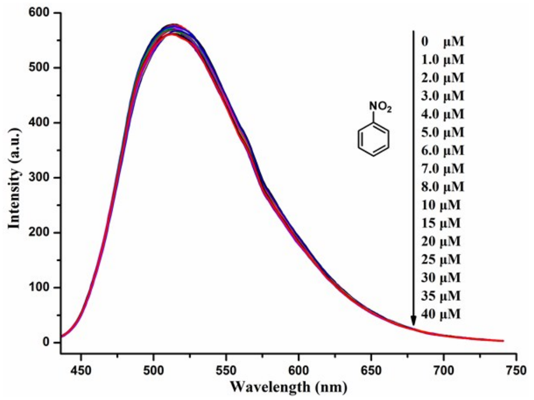
Intensity (a.u.)
Wavelength (nm)
0
100
200
300
400
500
600
450
500
550
600
650
700
750
NO2
0 μM
1.0 μM
2.0 μM
3.0 μM
4.0 μM
5.0 μM
6.0 μM
7.0 μM
8.0 μM
10 μM
15 μM
20 μM
25 μM
30 μM
35 μM
40 μM

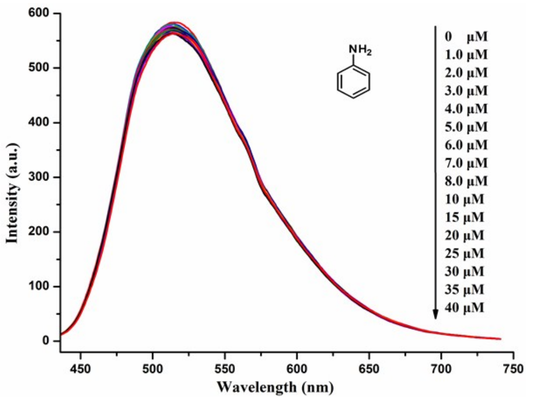
Intensity (a.u.)
Wavelength (nm)
0
100
200
300
400
500
600
450
500
550
600
650
700
750
NH2
0 μM
1.0 μM
2.0 μM
3.0 μM
4.0 μM
5.0 μM
6.0 μM
7.0 μM
8.0 μM
10 μM
15 μM
20 μM
25 μM
30 μM
35 μM
40 μM

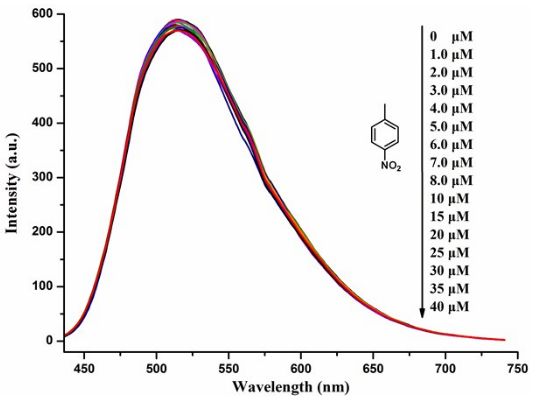
Intensity (a.u.)
Wavelength (nm)
0
100
200
300
400
500
600
450
500
550
600
650
700
750
NO2
0 μM
1.0 μM
2.0 μM
3.0 μM
4.0 μM
5.0 μM
6.0 μM
7.0 μM
8.0 μM
10 μM
15 μM
20 μM
25 μM
30 μM
35 μM
40 μM

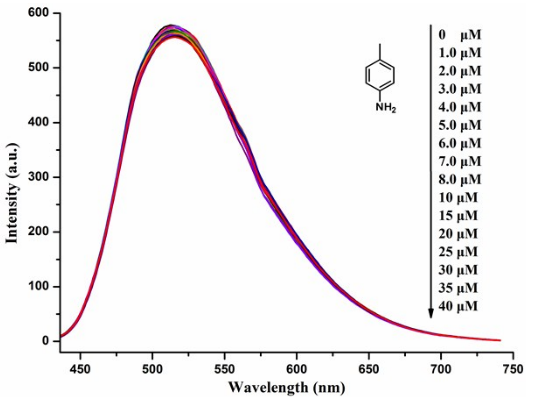
Intensity (a.u.)
Wavelength (nm)
0
100
200
300
400
500
600
450
500
550
600
650
700
750
NH2
0 μM
1.0 μM
2.0 μM
3.0 μM
4.0 μM
5.0 μM
6.0 μM
7.0 μM
8.0 μM
10 μM
15 μM
20 μM
25 μM
30 μM
35 μM
40 μM

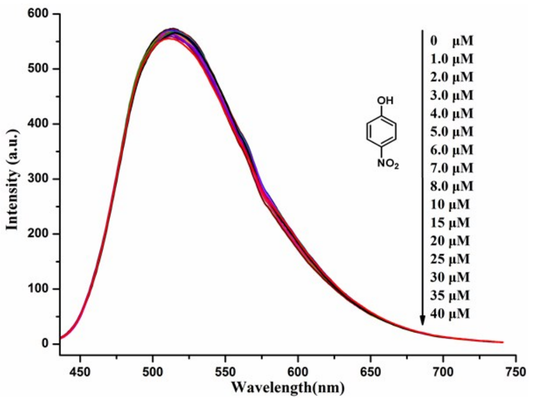
Intensity (a.u.)
Wavelength(nm)
0
100
200
300
400
500
600
450
500
550
600
650
700
750
OH
NO2
0 μM
1.0 μM
2.0 μM
3.0 μM
4.0 μM
5.0 μM
6.0 μM
7.0 μM
8.0 μM
10 μM
15 μM
20 μM
25 μM
30 μM
35 μM
40 μM

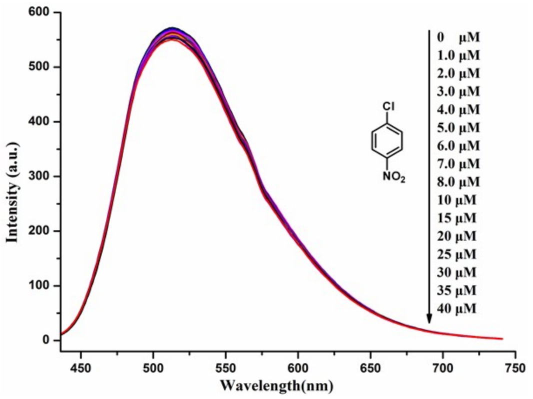
Intensity (a.u.)
Wavelength(nm)
0
100
200
300
400
500
600
450
500
550
600
650
700
750
Cl
NO2
0 μM
1.0 μM
2.0 μM
3.0 μM
4.0 μM
5.0 μM
6.0 μM
7.0 μM
8.0 μM
10 μM
15 μM
20 μM
25 μM
30 μM
35 μM
40 μM

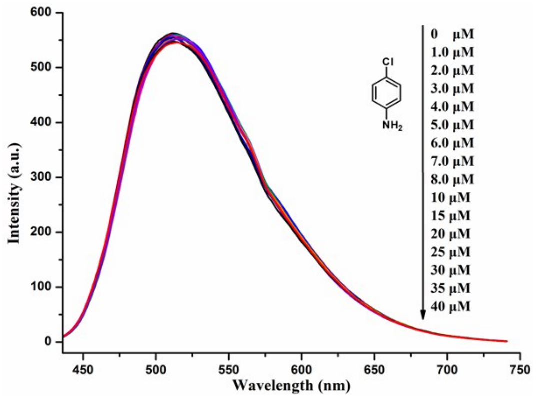
Intensity (a.u.)
Wavelength (nm)
0
100
200
300
400
500
600
450
500
550
600
650
700
750
Cl
NH2
0 μM
1.0 μM
2.0 μM
3.0 μM
4.0 μM
5.0 μM
6.0 μM
7.0 μM
8.0 μM
10 μM
15 μM
20 μM
25 μM
30 μM
35 μM
40 μM

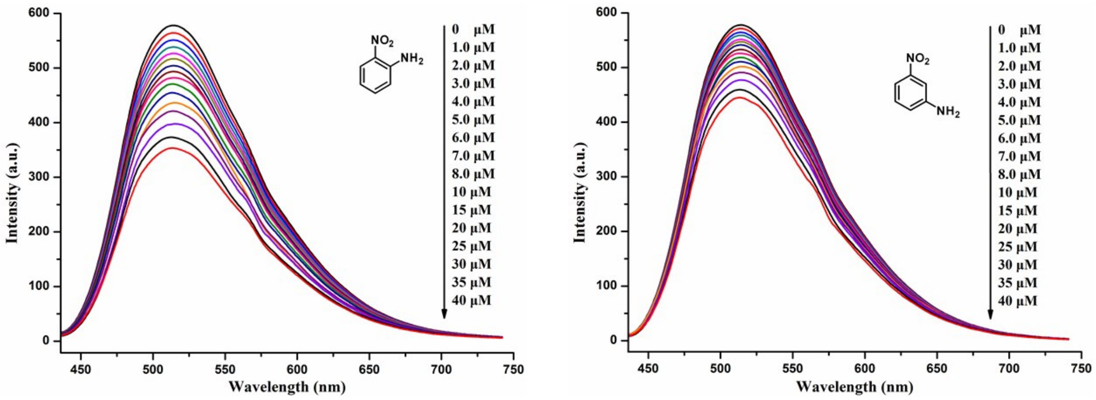

Figure S10 Fluorescence spectra of PTPTB suspension in DMF in the presence of different concentrations of toluene, nitrobenzene, aniline, *p*-nitrotoluene, *p*-aminotoluene, *p*-nitrophenol, *p*-chloronitrobenzene, *p*-chloroaniline, *o*-nitroaniline and *m*-nitroaniline.

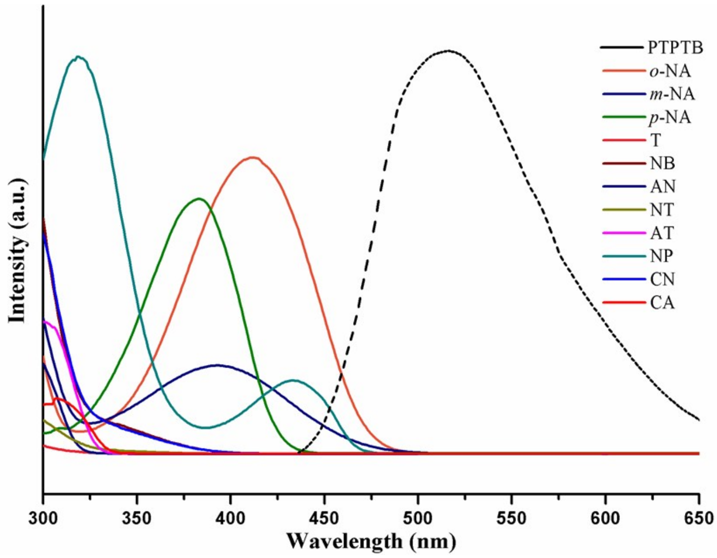

Figure S11 Spectral overlap between the absorption spectra of aromatic analytes and the emission spectrum of PTPTB in DMF.

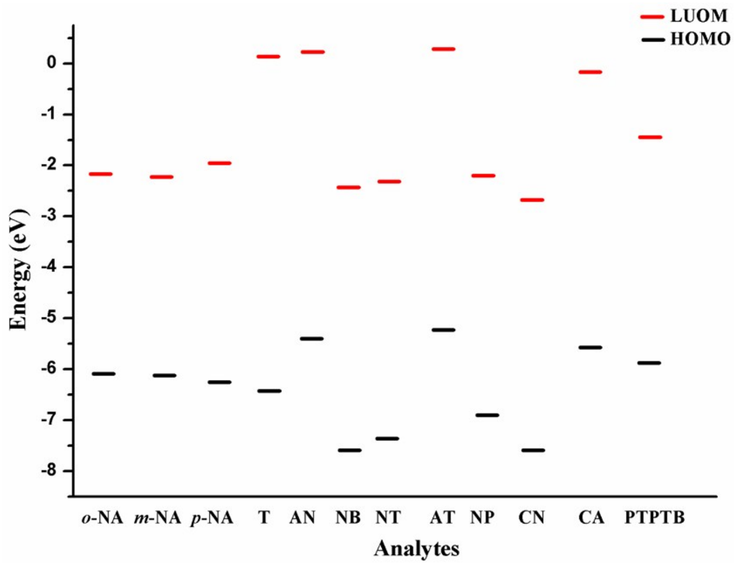

Figure S12 HOMO and LUMO profiles for PTPTB and aromatic analytes.

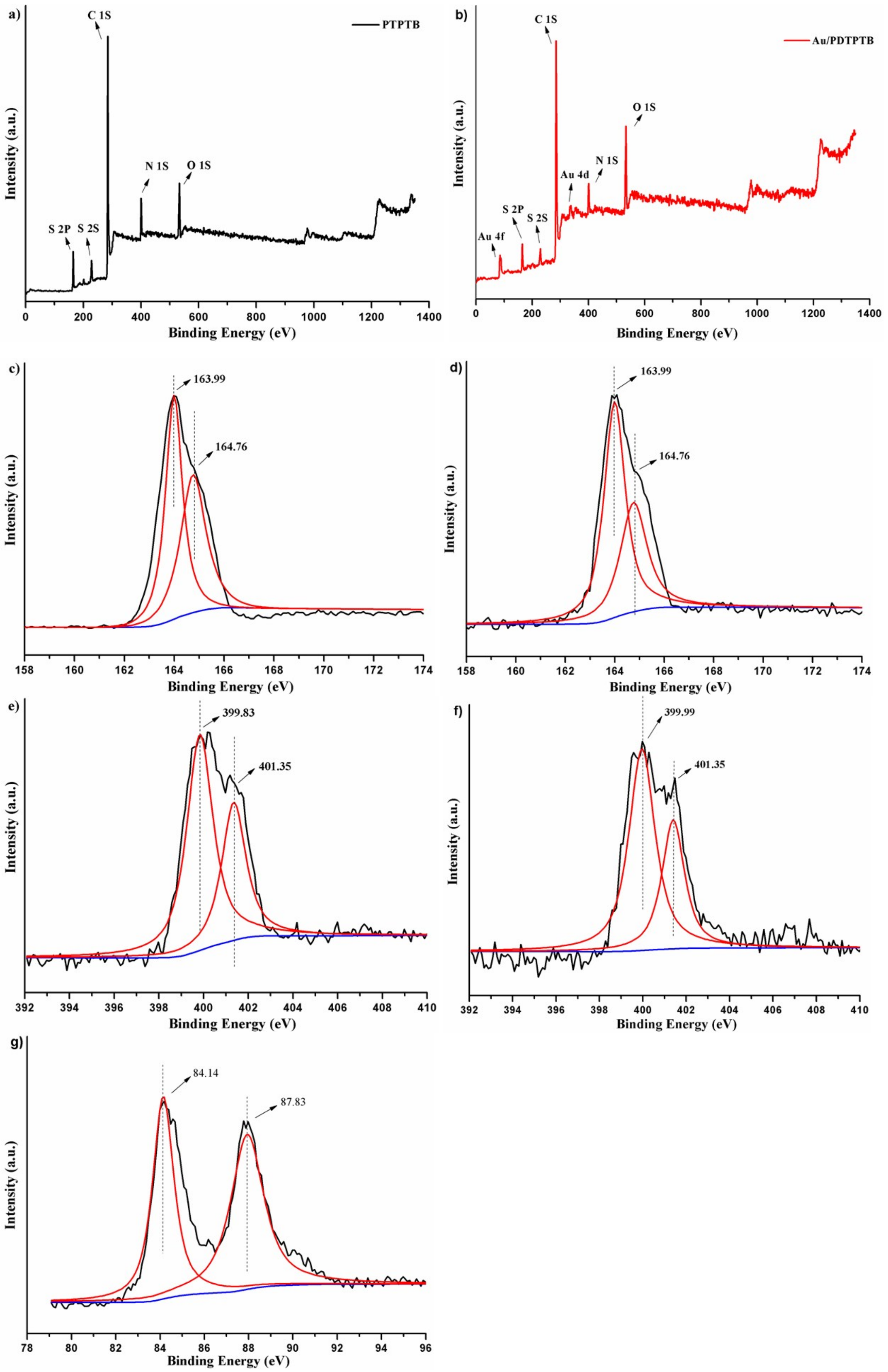

Figure S13 XPS analysis of PDTPTB and Au/PDTPTB. Survey scan of a) PDTPTB and b) Au/PDTPTB; c) S 2p and e) N 1s XPS spectra for PDTPTB; d) S 2p and f) N 1s XPS spectra for Au/PDTPTB. g) high-resolution Au 4f spectra for Au/PDTPTB.

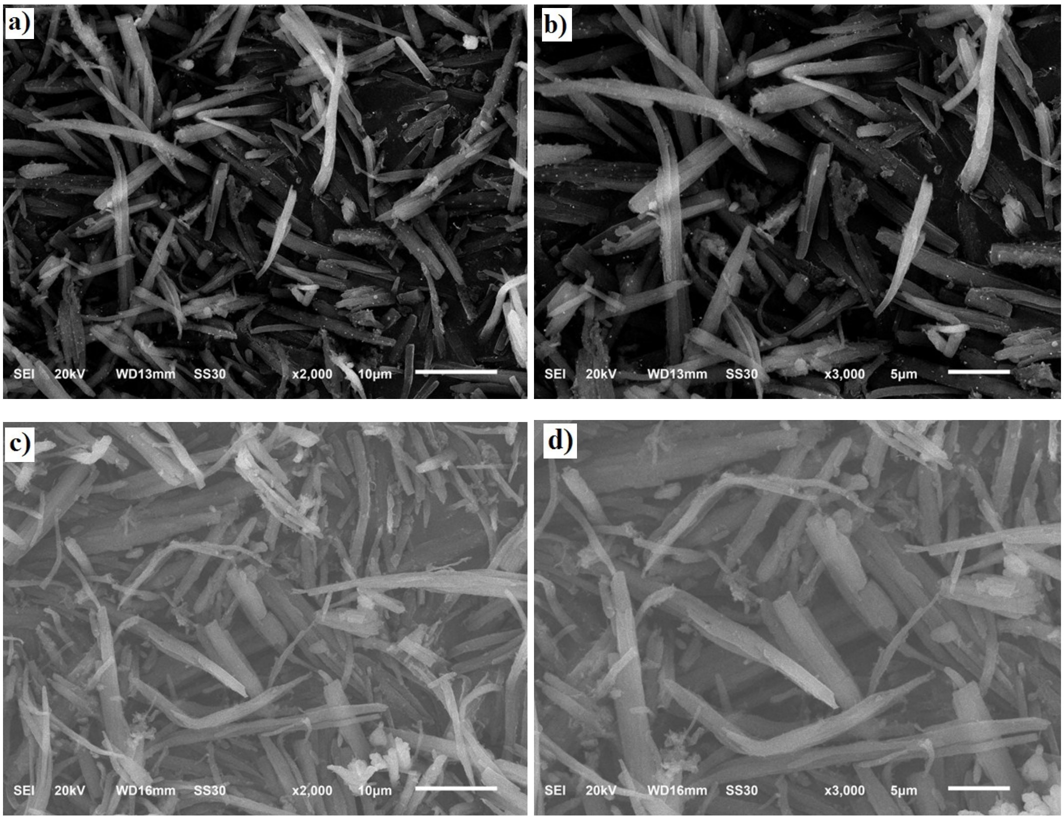

Figure S14 SEM images of (a, b) Au/PTPTB before use and (c, d) Au/PTPTB after six runs of catalytic reactions.

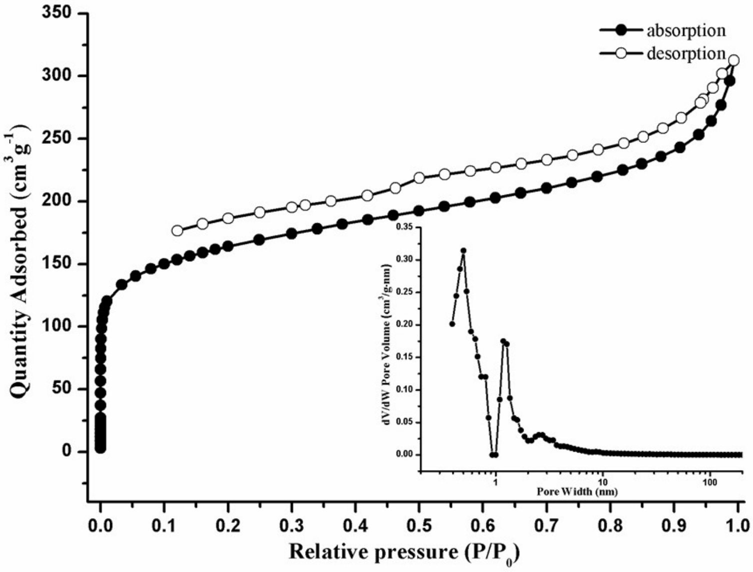

Figure S15 Nitrogen sorption isotherms of Au/PTPTB. Inset: pore-size distribution profile calculated by using the DFT method.

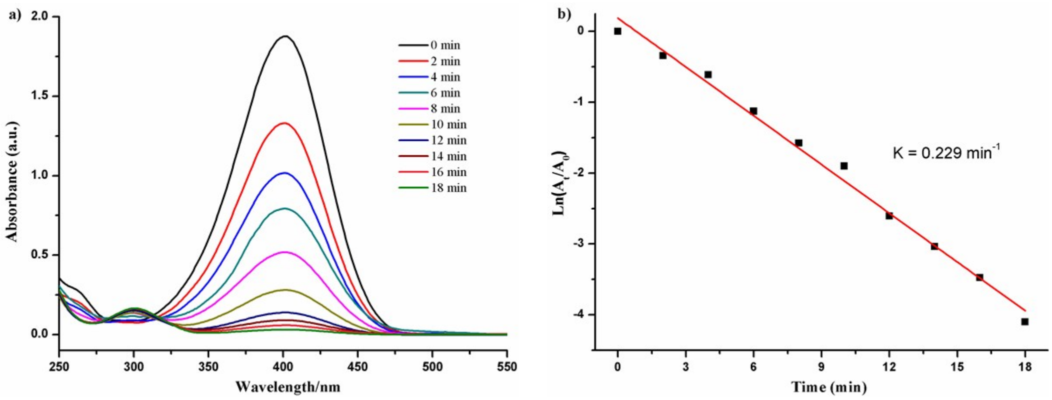

Figure S16 (a) Time-dependent UV-Vis absorption spectra for the reduction of *p*-NP with $NaBH_4$ in the presence of $HAuCl_4$. (c) Plot of the $\ln[C_t/C_0]$ versus reaction time for the Au NPs catalyzed reduction of *p*-NP.

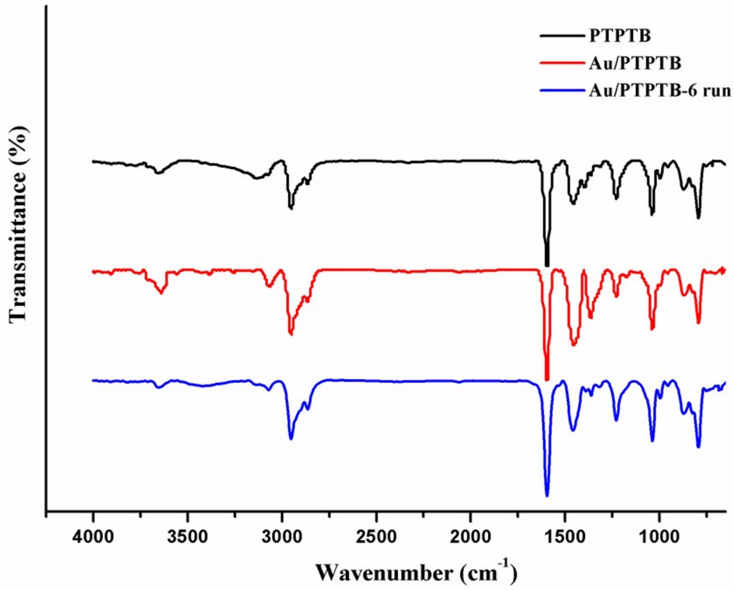

Figure S17 FT-IR spectra of PTPTB, Au/PTPTB and Au/PTPTB-6 run (after six runs of catalytic reactions).

Table S1: A comparative account of *p*-NA detection by fluorescent materials.

Sr. No.	Material	Quenching constant (M^{-1})	Sensitivity	Reference No.
1	TPDC-DB	1.7×10^4	455 ppb	S2
2	Zn MOF	-	4 ppm	S3
3	Zn MOF	2.18×10^4	-	S4
4	Eu MOF	6.6×10^3	-	S5
5	Cd MOF	40787	20 µM	S6
6	Cd MOF	9.8×10^4	0.01875 mM	S7
7	Nitrogen-doped carbon dots	1.25×10^4	1×10^{-7} M	S8
8	Phenanthro[4,5-fgh]-pyrido[2,3-b]quinoxaline	1.07×10^5	0.03 ppm	S9
9	Calix[4]arene	2.06×10^4	-	S10
10	Pyrene and 1-methylpyrene	1.7×10^4	-	S11
11	PTPTB	7.08×10^4	4.2×10^{-6} M	**This work**

Table S2: HOMO and LUMO energies calculated for PTPTB and aromatic analytes.

Compound	HOMO map	LUMO map	HOMO (eV)	LUMO (eV)	E_g (eV)[a]
PTPTB		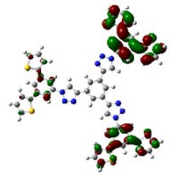	-5.87	-1.45	4.42
4-NA	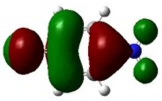	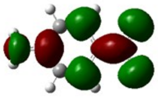	-6.25	-1.95	4.30
3-NA	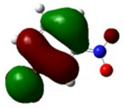	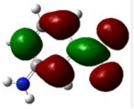	-6.14	-2.24	3.90
2-NA	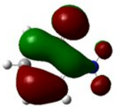	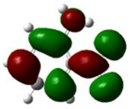	-6.06	-2.17	3.89
T	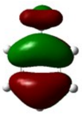	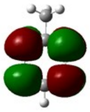	-6.40	0.15	6.55
A	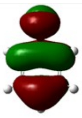	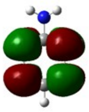	-5.39	0.25	5.64
NB	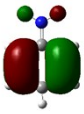	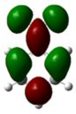	-7.59	-2.43	5.16
4-MA	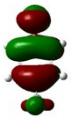	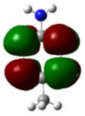	-5.23	0.27	5.50
MNB	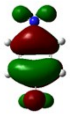	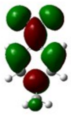	-7.36	-2.32	5.04
4-CA	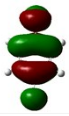	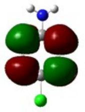	-5.57	-0.19	5.38
CNB	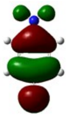	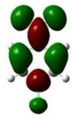	-7.57	-2.67	4.90
4-NP	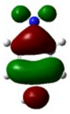	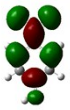	-6.92	-2.22	4.70
NMNA	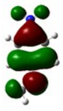	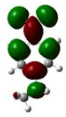	-5.97	-1.85	4.13

a) LUMO = HOMO-E_g

Table S3. Literature reported rate constants of other similar 4-nitrophenol reduction reactions catalyzed by Au-based catalysts.

Sr. No.	Catalyst	Yield (%)	Time (min)	Rate constant (min^{-1})	Reference No.
1	Fe_3O_4@SiO_2-LBL-Au(0)	95	12	0.18	S12
2	γ-Fe_2O_3@mSiO_2-SH-Au	99	6	0.32	S13
3	Mn@SiO_2_NH_2@Au	97	12	0.366	S14
4	HP5@AuNPs-0.5	-	7	0.38	S15
5	Au@CeO2–ZrO2-500°C DP-Au/CeO2–ZrO2-500°C	- -	7 4	0.57 0.89	S16
6	Au(0)@TpPa-1	-	13	0.111	S17
7	Au@CPF-1	99	12	0.303	S18
8	Au/TAPB-DMTP-COF	100	10	0.46	S19
9	Au@MIL-100(Fe)	-	15	0.33	S20
10	Au@UiO-66(NH_2)	100	9	0.45	S21
11	AuNPs	100	4.7	0.54	S22
12	Au/PTPA	98	4.5	0.443	S23
13	Au/PTPTB	99	4	0.812	**This work**

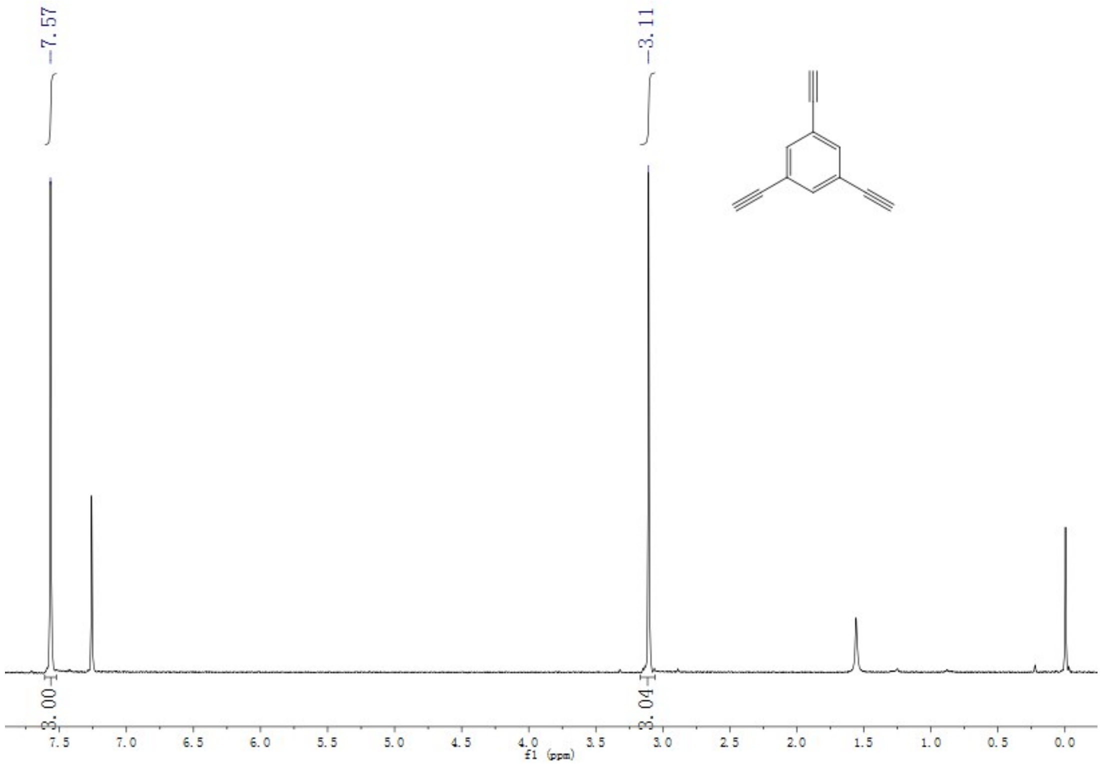

Figure S18 ^{1}H NMR spectrum of **1** conducted in CDCl$_3$.

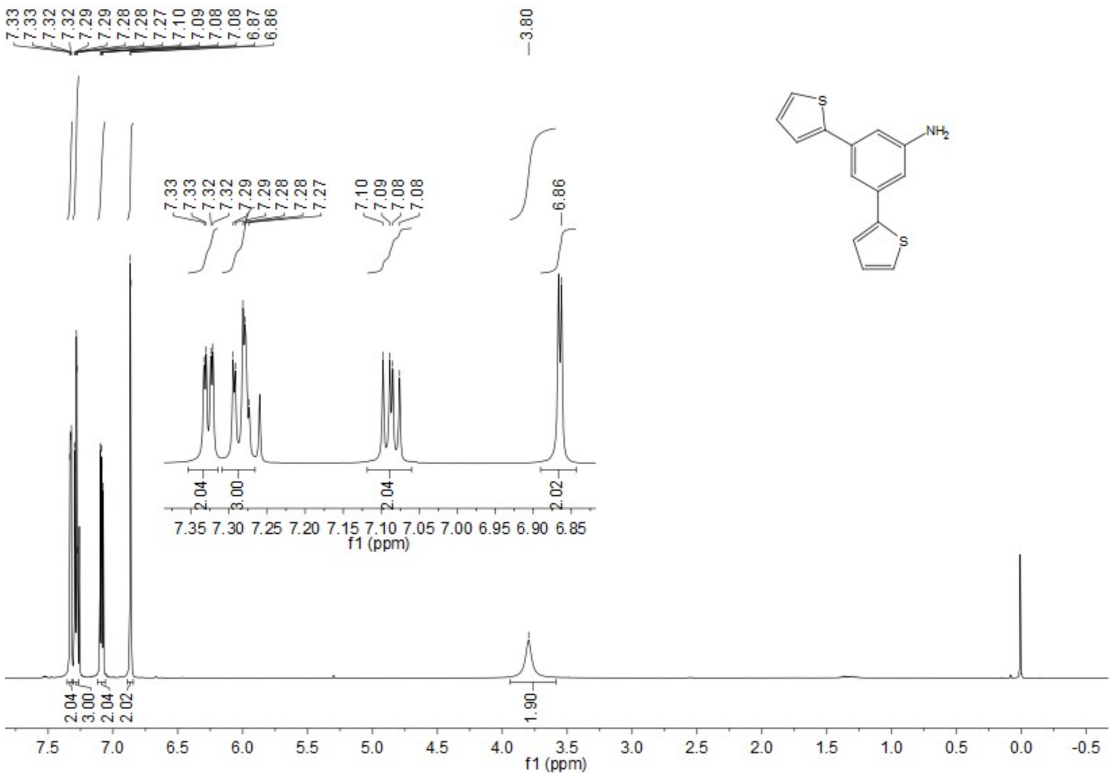

Figure S19 ^{1}H NMR spectrum of **1** conducted in CDCl$_3$.

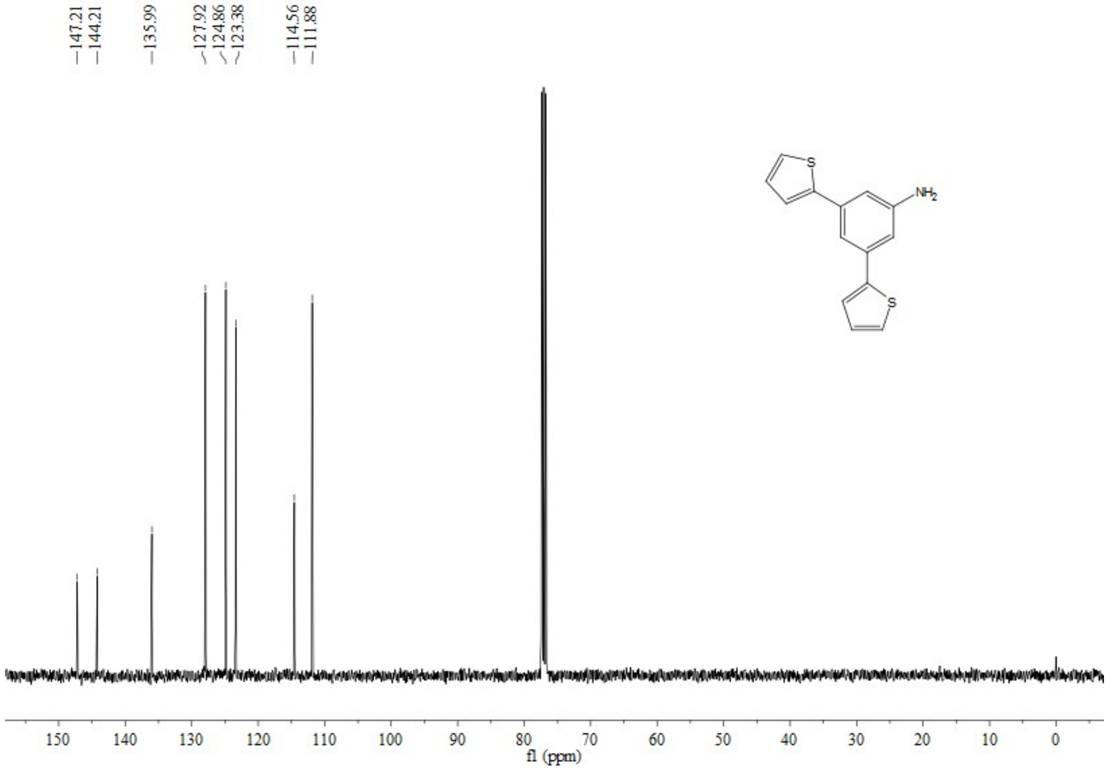

Figure S20 ^{13}C NMR spectrum of **1** conducted in CDCl$_3$.

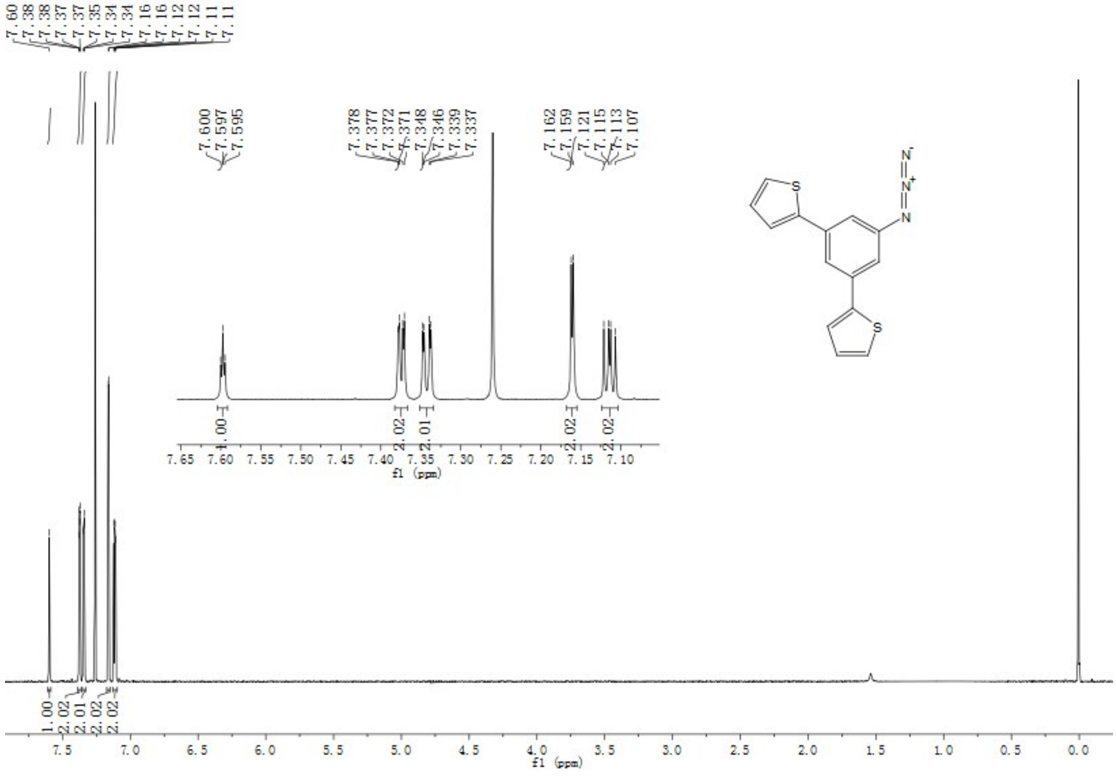

Figure S21 ^{1}H NMR spectrum of **2** conducted in CDCl$_3$.

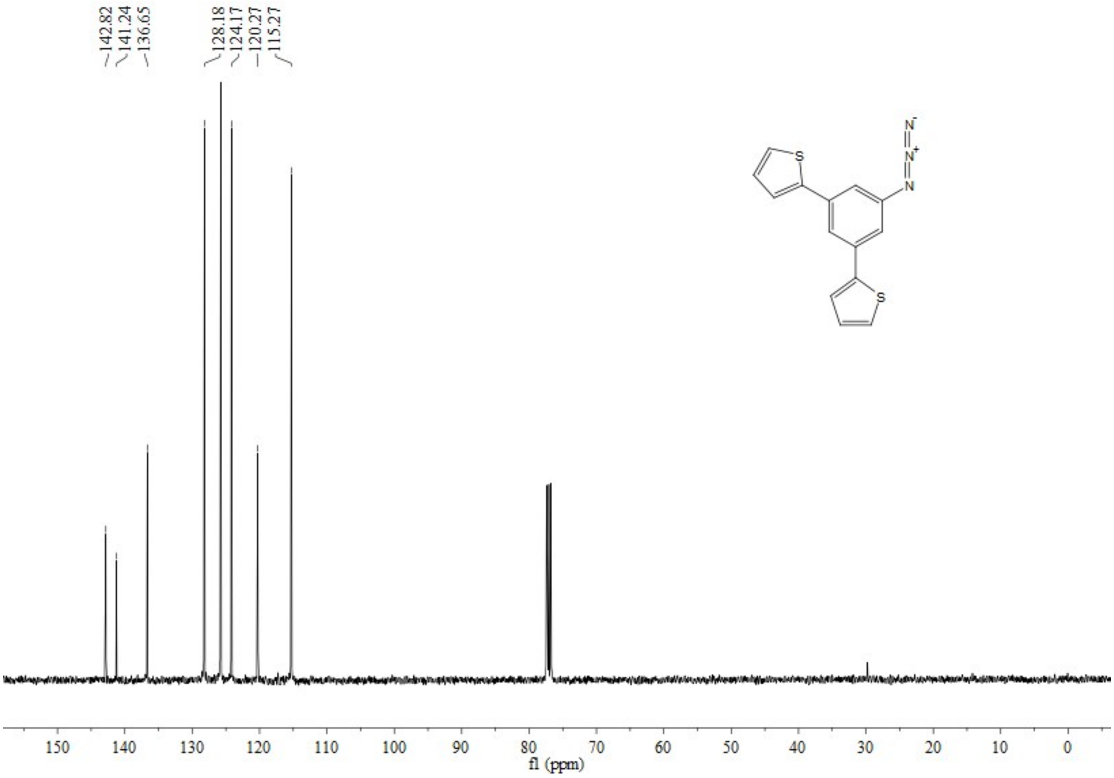

Figure S22 ^{13}C NMR spectrum of **2** conducted in $CDCl_3$.

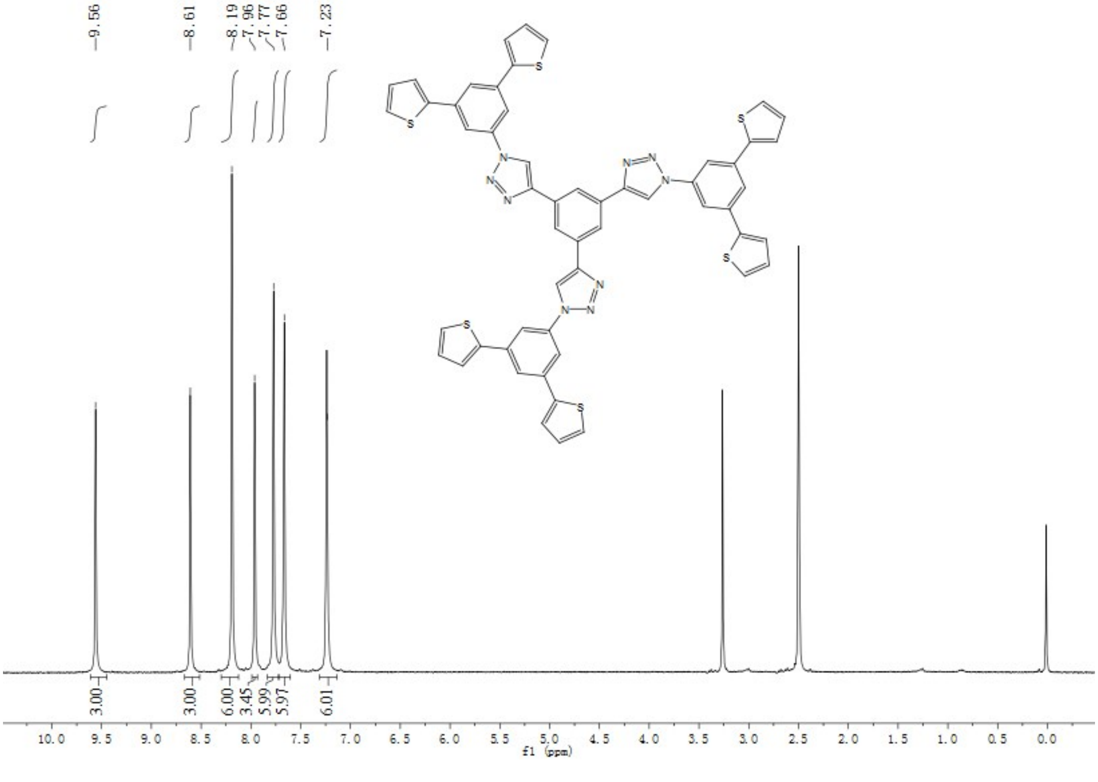

Figure S23 ^{1}H NMR spectrum of **TPTB** conducted in DMSO-d_6.

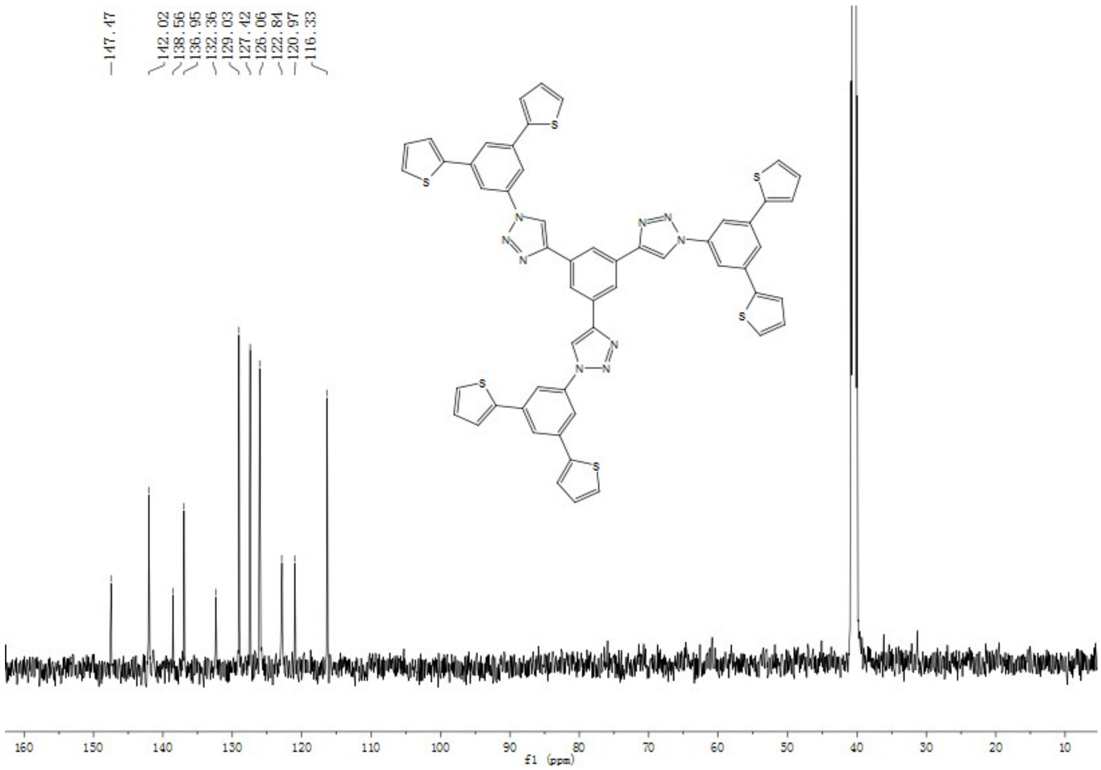

Figure S24 ^{13}C NMR spectrum of **TPTB** conducted in DMSO-d_6.

References

[S1] S. H. Lim, Y. X. Su and S. M. Cohen, *Angew. Chem. Int. Ed.*, 2012, **51**, 5106-5109.

[S2] A. Deshmukh, S. Bandyopadhyay, A. James and A. Patra, *J. Mater. Chem. C*, 2016, **4**, 4427-4433.

[S3] X. Y. Wan, F. L. Jiang, C. P. Liu, K. Zhou, L. Chen, Y. L. Gai, Y. Yang and M. C. Hong, *J. Mater. Chem. A*, 2015, **3**, 22369-22376.

[S4] Z. C. Yu, F. Q. Wang, X. Y. Lin, C. M. Wang, Y. Y. Fu, X. J. Wang, Y. N. Zhao and G. D. Li, *J. Solid State Chem.*, 2015, **232**, 96-101.

[S5] F. Wang, C. Wang, Z. Yu, Q. He, X. Li, C. Shang and Y. Zhao, *RSC Adv.*, 2015, **5**, 70086-70093.

[S6] P. Y. Wu, Y. H. Liu, Y. Li, M. Jiang, X. L. Li, Y. H. Shi and J. Wang, *J. Mater. Chem. A*, 2016, **4**, 16349-16355.

[S7] Y. J. Yang, M. J. Wang and K. L. Zhang, *J. Mater. Chem. C*, 2016, **4**, 11404-11418.

[S8] H. R. Yuan, D. N. Li, Y. Liu, X. Z. Xu and C. X. Xiong, *Analyst*, 2015, **140**, 1428-1431.

[S9] P. Singla, P. Kaur and K. Singh, *Tetrahedron Lett.* 2015, **56**, 2311-2314.

[S10] J. Zhan, X. Zhu, F. Fang, F. Miao, D. Tian and H. Li, *Tetrahedron*, 2012, **68**, 5579-5784.

[S11] C. E. Agudelo-Morales, O. F. Silva, R. E. Galian and J. Pérez-Prieto, *ChemPhysChem*, 2012, **13**, 4195-4201.

[S12] Y. H. Zhu, J. H. Shen, K. F. Zhou and C. Chen, *J. Phys. Chem. C.*, 2011, **115**, 1614-161.

[S13] X. Z. Li, X. H. Zhu and R. Li, *J. Mater. Chem. A*, 2014, 2, 10485-10491.

[S14] M. Rocha, C. Fernandes and C. Pereira, *RSC Adv.*, 2015, **5**, 5131-5141.

[S15] G. F. Zhao, X. Ran, X. Zhou, X. P. Tan, H. Lei, X. G. Xie, L. Yang and G. B. Du, *ACS Sustainable Chem. Eng.*, 2018, **6**, 3938-3947.

[S16] C. H. Du, Y. Guo, Y. L. Guo, X. Q. Gong and G. Z. Lu, *J. Mater. Chem. A*, 2017, **5**, 5601-5611.

[S17] P. Pachfule, S. Kandambeth, D. D. Díaz and R. Banerjee, *Chem. Commun.*, 2014, **50**, 3169-3172.

[S18] Z. D. Ding,Y. X Wang and S. F Xi, *Chem. -Eur. J.*, 2016, 22, 17029-17036.

[S19] X. F. Shi, Y. J. Yao, L. F. Chi and G. Lu, *ACS Appl. Mater. Interfaces*, 2017, **9**, 7481-7488.

[S20] F. Ke, J. F. Zhu, L. J. Qiu and X. Jiang, *Chem. Commun.*, 2013, **49**, 1267-1269.

[S21] Y. Luan, Y. Qi, H. Gao, N. Zheng and G. Wang, *J. Mater. Chem. A*, 2014, **2**, 20588-20596.

[S22] C. Deraedt, L. Salmon, J. Ruiza and D. Astruc, *Chem. Commun.*, 2014, **50**, 14194-14196.

[S23] F. Wei, C. F. Lu, F. Y. Wang, G. C. Yang, Z. X. Chen and J. Q. Nie, *Mater. Lett.*, 2018, **212**, 251-255.